Video Article

Sequential Application of Glass Coverslips to Assess the Compressive Stiffness of the Mouse Lens: Strain and Morphometric Analyses

Catherine Cheng[1], David S. Gokhin[1], Roberta B. Nowak[1], Velia M. Fowler[1]

[1]Department of Cell and Molecular Biology, The Scripps Research Institute

Correspondence to: Velia M. Fowler at Velia@scripps.edu

URL: http://www.jove.com/video/53986
DOI: doi:10.3791/53986

Keywords: Cellular Biology, Issue 111, lens mechanics, strain, eye, aging, lens nucleus, morphometrics, compression, biomechanics

Date Published: 5/3/2016

Citation: Cheng, C., Gokhin, D.S., Nowak, R.B., Fowler, V.M. Sequential Application of Glass Coverslips to Assess the Compressive Stiffness of the Mouse Lens: Strain and Morphometric Analyses. *J. Vis. Exp.* (111), e53986, doi:10.3791/53986 (2016).

Abstract

The eye lens is a transparent organ that refracts and focuses light to form a clear image on the retina. In humans, ciliary muscles contract to deform the lens, leading to an increase in the lens' optical power to focus on nearby objects, a process known as accommodation. Age-related changes in lens stiffness have been linked to presbyopia, a reduction in the lens' ability to accommodate, and, by extension, the need for reading glasses. Even though mouse lenses do not accommodate or develop presbyopia, mouse models can provide an invaluable genetic tool for understanding lens pathologies, and the accelerated aging observed in mice enables the study of age-related changes in the lens. This protocol demonstrates a simple, precise, and cost-effective method for determining mouse lens stiffness, using glass coverslips to apply sequentially increasing compressive loads onto the lens. Representative data confirm that mouse lenses become stiffer with age, like human lenses. This method is highly reproducible and can potentially be scaled up to mechanically test lenses from larger animals.

Video Link

The video component of this article can be found at http://www.jove.com/video/53986/

Introduction

The lens is a transparent and avascular organ in the anterior chamber of the eye that is responsible for fine focusing of light onto the retina. A clear basement membrane, called the lens capsule, surrounds a bulk of elongated fiber cells covered by an anterior monolayer of epithelial cells[1,2]. Life-long growth of the lens depends on the continuous proliferation and differentiation of epithelial cells at the lens equator into new fiber cells that are added onto previous generations of fiber cells in a concentric manner[2]. Over time, lens fiber cells undergo compaction, resulting in a rigid center in the middle of the lens called the nucleus[1]. Accommodation, defined as a dioptric change in the optical power of the eye, occurs in humans when the ciliary muscles contract to deform the lens and allow a true increase in optical power to focus on near objects[3-5]. In the unaccommodated eye, the lens is held in a relatively flattened state due to tension from zonular fibers. When the ciliary muscles contract, the tension on the lens is released, leading to decreased lens equatorial diameter and increased axial thickness. Age-related changes in the lens cause presbyopia, a progressive loss of lens accommodation, which leads to the need for reading glasses.

Several studies have linked presbyopia to age-related increase in the intrinsic stiffness of the lens[6-11]. Stiffness is defined as the resistance of an elastic object to deform under applied load. A variety of methods have been used to examine stiffness of human lenses, including spin compression[12-14], actuator compression[15], probe indentation[16], dynamic mechanical analysis [6,10] and bubble-based acoustic radiation force[17]. While mouse lenses do not accommodate or develop presbyopia, mouse models for lens pathologies are valuable tools because mice are less expensive than larger animals, well characterized genetically and undergo accelerated age-related changes due to rapid aging. A handful of studies have examined mouse lens stiffness with compression methods and demonstrated changes in lens stiffness due to aging or targeted genetic disruptions[18-21]. Thus, mouse lenses are good models for studying age-related changes in lens stiffness.

This protocol describes a simple and inexpensive, yet precise and reproducible, compression method for determining mouse lens stiffness based on application of glass coverslips onto the lens in conjunction with photographing the lens through a dissection microscope and mirror. This method yields robust strain and morphometric data with an easily fabricated and assembled apparatus. The representative results confirm that mouse lenses increase in stiffness with age.

Protocol

All animal procedures were performed in accordance with recommendations in the Guide for the Care and Use of Laboratory Animals by the National Institutes of Health and under an approved protocol by the Institutional Animal Care and Use Committee at The Scripps Research Institute.

1. Lens Dissection

1. Euthanize mice according to recommendations in the National Institutes of Health "Guide for the Care and Use of Laboratory Animals" and approved institution animal use protocols.
2. Enucleate the eye from mice using curved forceps. Depress the tissue around the eye with the forceps to bring the eye out of the socket, and then pluck the eye from the socket with the forceps. Transfer eyes to fresh 1x phosphate buffered saline (PBS) in dissection dish.
3. Cut off the optic nerve as close to the eyeball as possible. Gently and carefully insert fine straight tweezers into the eyeball through the hole where the optic nerve exits the posterior.
4. Carefully make an incision with scissors into the eyeball from the posterior to the edge of the cornea. Rodent lenses occupy ~30% of the eye. Make these incisions carefully, and do not insert tweezers or scissors too deep into the eye to avoid damaging the lens.
5. Cut along the junction between the cornea and sclera at least half way around the eyeball.
6. Gently push on the cornea to remove the lens from the eye through the opening made in steps 1.4 and 1.5.
7. Use fine tip straight forceps to carefully remove any large debris that is still attached to the lens. Visually inspect the lens for any damage before proceeding to the stiffness measurements.

2. Stiffness Measurements

1. Weigh at least 10 coverslips from the same box using an analytical balance. Find the average weight of the coverslips. For consistency, use the same box of coverslips for all experiments. Pre-wet the coverslips and right-angle mirror in 1x PBS at room temperature for at least 2 hr before starting experiments.
2. Fill the measurement chamber (see **Figure 1**) with 65 - 75 ml of 1x PBS. The measurement chamber was made out of Plexiglas by an in-house machine shop, and divots in the chamber were made by a drill press set to the desired depth with an appropriate drill bit. Lenses remain transparent in 1x PBS at room temperature for the duration of mechanical testing.

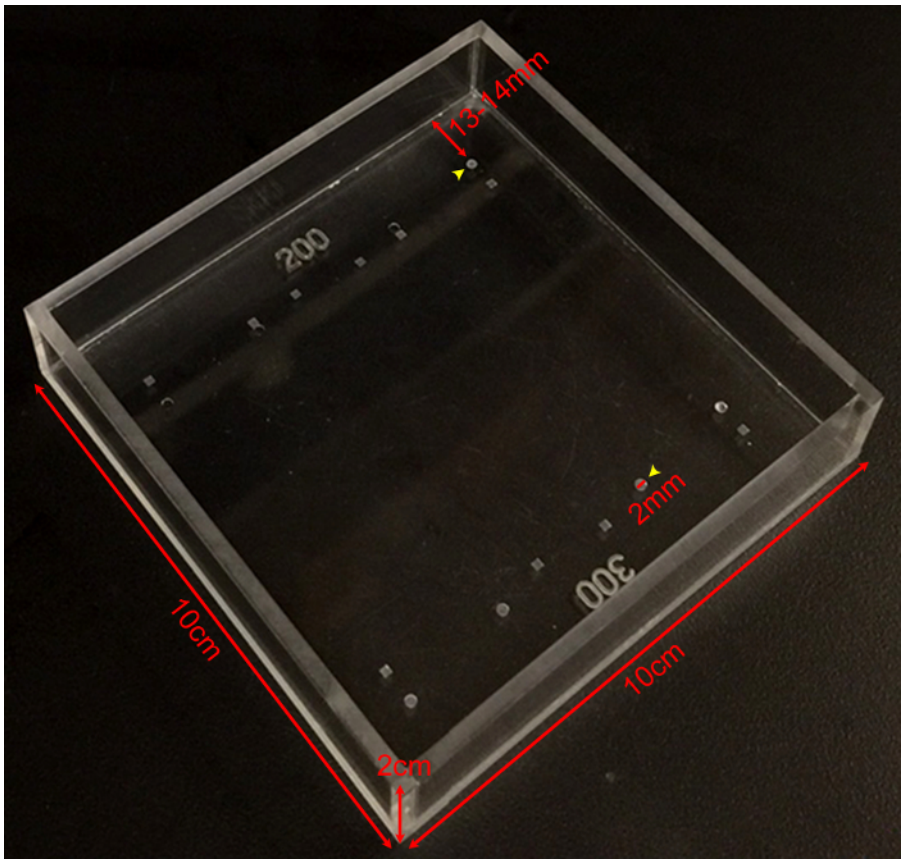

Figure 1: Stiffness Measurement Chamber. A photo showing the dimensions of the custom-made stiffness measurement chamber with a variety of divots of different depths and shapes. The round divots that are 200 µm or 300 µm deep (yellow arrowheads) are used for the measurements on mouse lenses. Divots are 2 mm in diameter and ~13 - 14 mm from the edge of the chamber. Please click here to view a larger version of this figure.

3. Place right-angle mirror into the chamber at a constant distance from the divot that will be used to hold the lens. Make sure the mirror does not move during the experiment.
4. Transfer dissected lenses to measurement chamber carefully with seizing forceps or curved forceps.
5. Take a top-view picture of the unloaded lens from directly overhead. Take mouse lens photos at 30X magnification with illumination from dissecting microscope (bottom) and a fiber optic light source on the left and right sides. Set the fiber optic power supply to 80% of the maximum light intensity. Adjust the power supply output based on ambient lighting, user preference and picture quality as needed.

6. Take a side-view picture of the unloaded lens, which can be seen through the right-angle mirror. If camera is not calibrated, take a picture of the mirror edge in focus. The mirror edge is 5 mm long, and this measurement can later be used to determine the pixels/mm and serve as a scale bar in the images.
7. Place lens into the divot, and confirm that the lens is seated securely and straight in the divot. Take a picture of the lens before loading. The lens should be resting in the divot on its anterior or posterior pole.
8. Place 1 coverslip gently onto the lens. Wait 2 min to permit creep, and take another side-view picture of the loaded lens.
9. Continue adding coverslips as in step 2.8 and taking side-view pictures after the addition of each coverslip as in step 2.8 until a total of 10 coverslips are applied.
10. Remove all coverslips. Wait 2 min, and take a side-view picture of the lens (inside and outside of the divot) after removing all coverslips.

3. Lens Nucleus Measurement

1. To determine the lens nucleus size, move the lens to a clean Petri dish filled with 1x PBS.
2. Gently decapsulate the lens using fine straight forceps.
3. Slough off the cortical fiber cells by rolling the lens between gloved fingers. The remaining lens nucleus will feel like a hard marble. Use this procedure to isolate the nucleus on adult lenses starting at 1 month of age. Since the isolated nucleus is a rigid body, further mechanical testing of the lens nucleus cannot be performed using this described method.
4. Gently rinse the lens nucleus in 1x PBS in the Petri dish.
5. Place the lens nucleus back into the measurement chamber (not in the divot), and take an image of the lens nucleus through the right-angle mirror.

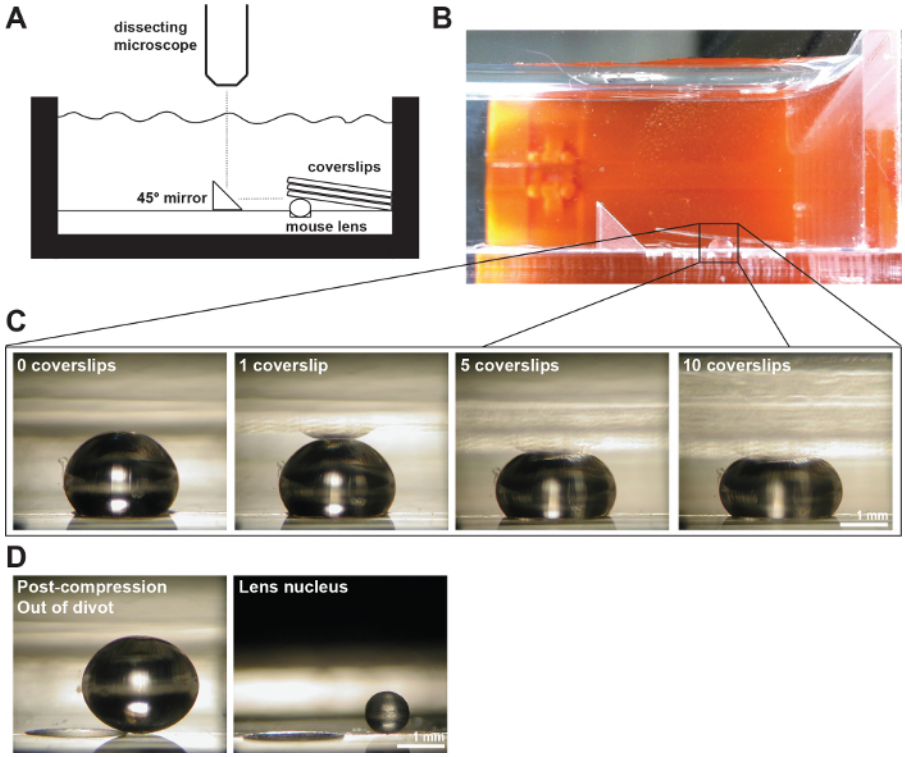

Figure 2: A Mouse Lenses Compressed by Coverslips. (A) Schematic and (B) photograph of the experimental setup showing a 2-month-old mouse lens in a 200-µm-deep divot in the measurement chamber filled with 1x PBS. A right angle mirror and a digital camera mounted on a dissection microscope were used to collect images of the lens during compression by coverslips. (C) Photos of sagittal views of a 2-month-old wild-type lens compressed by successively increasing numbers of coverslips provided the raw data for measuring axial and equatorial diameters and calculating axial and equatorial strains during coverslip-based compression testing. A reflection of the lens can sometimes be seen in the coverslips (most clearly visible in the 1 coverslip image). When making measurements, ignore the reflection and measure to the apex of the lens. (D) Photos of sagittal views of the 2-month-old wild-type lens post-compression and the isolated lens nucleus. The post-compression lens and isolated nucleus are sitting outside of the divot. Scale bars, 1 mm. This figure is modified from Gokhin, *et al*. *PloS one*, 2012[19]. Please click here to view a larger version of this figure.

4. Image Analysis

1. Measure equatorial and axial diameters of lenses before loading and after each loading step using ImageJ or similar software. Measure the diameter of each lens nucleus. The lens nucleus is nearly spherical so a measurement at any orientation will suffice[19,21].
2. Correct the lens axial diameters by adding the depth of the divot used. In the measurement chamber, the divot obscured 200 µm (2-month-old mouse lenses) or 300 µm (4-month-old and 8-month-old mouse lenses) of the axial thickness of the lens.
3. Calculate the axial and equatorial strains from the lens diameter measurements using the equation, $\varepsilon = (d - d_0) / d_0$, where ε is strain, d is the axial or equatorial diameter at a given load, and d_0 is the corresponding axial or equatorial diameter at zero load.

4. Plot the axial and equatorial strains as functions of the imposed load (in mg).
5. Plot the axial, equatorial and nuclear diameters. Calculate and plot the lens aspect ratio by dividing the axial diameter by the equatorial diameter.
6. Calculate and plot the lens volume using the equation, volume = $4/3 \times \pi \times r_E^2 \times r_A$, where r_E is the equatorial radius and r_A is the axial radius measured from the picture taken in step 2.6. This equation assumes the lens is an oblate spheroid (ellipsoid)[1,22].
7. Calculate and plot the nuclear volume using the equation, volume = $4/3 \times \pi \times r_N^3$, where r_N is the radius of the lens nucleus as measured from the picture taken in step 3.5. This equation assumes the lens nucleus is a sphere[19,21].
8. Calculate and plot the nuclear fraction as the ratio of the nuclear volume to the lens volume.

Representative Results

The stiffness and dimensions of 2-, 4- and 8-month-old mouse lenses were measured. Mice were all wild-type animals on a pure C57BL6 strain background obtained from the TSRI Animal Breeding Facility, and each lens was loaded with 1 to 10 coverslips. The axial and equatorial strains were calculated as a function of applied load by measuring the axial and equatorial diameters of the lens after the addition of each coverslip, and then normalizing each change in diameter to the corresponding unloaded diameter. Eight lenses from each age were tested, and the results are expressed as the average ± standard error. As shown previously[19], axial strain is a logarithmic function of applied load (**Figure 3A**). There was a statistically significant age-dependent decrease in axial and equatorial strains under the maximum applied load (**Figure 3**), indicating that the mouse lens stiffens with age. Strain measurements were highly reproducible across lenses of the same age, as demonstrated by the small standard errors.

The image data collected during this experiment were also used to determine several other lens morphological characteristics (**Figure 4**). As expected, axial and equatorial diameters and lens volume increased with age (**Figure 4A, 4B and 4D**). The aspect ratio indicates that the lens has a slightly larger equatorial diameter than axial diameter, and this parameter did not change with age (**Figure 4C**). The diameter, volume and fraction of the lens nucleus increased with age (**Figure 4E, 4F and 4G**). These results suggest that the lens nucleus remodels to increase in relative size as the lens ages.

This data show that mouse lenses increase in stiffness with age, similar to changes in aging human lenses[9,15]. These data also agree with previous observations made using a similar method[18] and by Brillouin optical microscopy[23] that mouse lenses increase in stiffness with age. Two other studies have used the described method to show that tropomodulin-1, an actin pointed-end capping protein, CP49, a beaded intermediate filament protein, and aquaporin 0 are needed to maintain lens stiffness[19,20]. With this method, the plethora of mouse models for lens pathologies and the accelerated aging of mice can be used to understand lens stiffness changes due to genetic variation and/or aging. This method can also be adapted for lenses from other species. The dimensions of the chamber used for these experiments are optimized for mouse lenses, but can easily be scaled up for lenses from larger species. In the future, it would be interesting to determine whether lens size scales with lens stiffness across species.

At the lowest load (1 coverslip, 129.3 mg), there was no obvious difference in axial and equatorial strains between 2-, 4- and 8-month-old lenses. The increase in lens stiffness with age became more apparent at higher loads. It is possible that the outermost cortex of the lens (~100 µm) that is compressed by first coverslip does not change in stiffness with age, or that this method is unable to distinguish small changes in strain at low loads. The morphometrics data indicate that increases in both the whole lens and nuclear volume correlate with increased lens stiffness as a function of age.

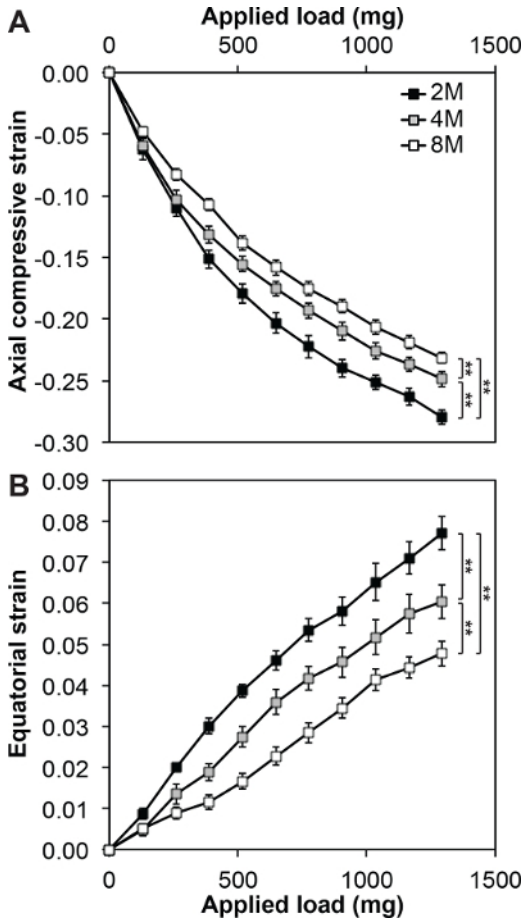

Figure 3: Axial and Equatorial Strain-load Curves for 2-, 4- and 8-month-old (2M, 4M and 8M) Wild-type Mouse Lenses. (A) Axial compressive strain plotted as a function of the applied load (mg). (B) Equatorial compressive strain plotted as a function of the applied load (mg). Four- and 8-month-old lenses exhibited less strain than 2-month-old lenses at equivalent maximum loads, indicating an increase in lens stiffness with age. **, p <0.01. Note that the Y-axis is different between (A) and (B). Please click here to view a larger version of this figure.

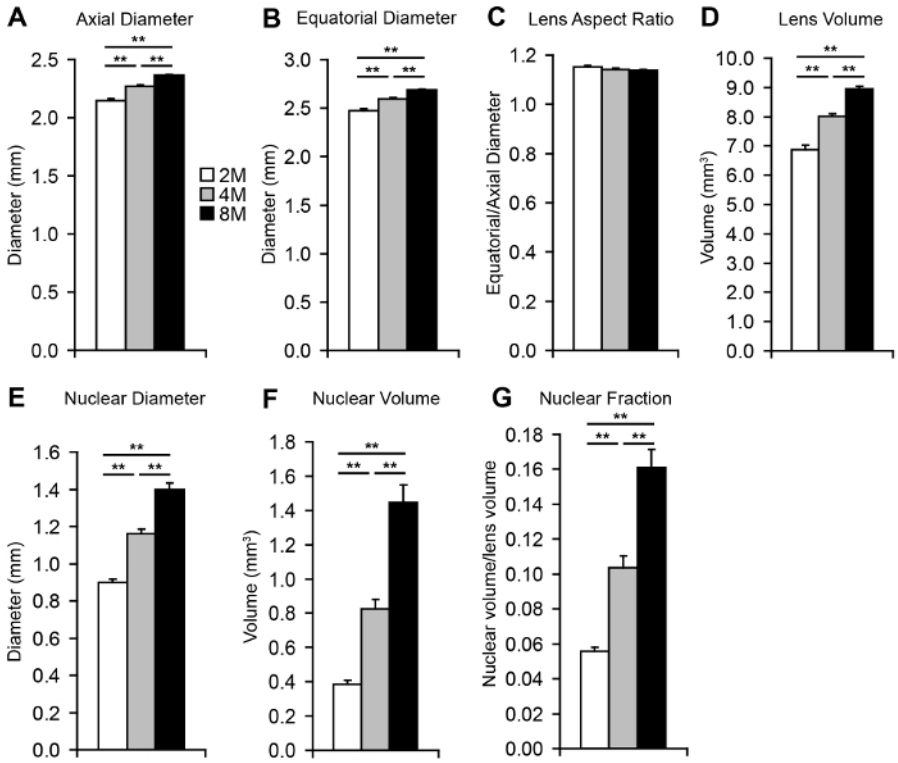

Figure 4: Morphological Characteristics of 2-, 4- and 8-month-old (2M, 4M and 8M) Wild-type Mouse Lenses. (A) Axial diameter and (B) equatorial diameter progressively increase with age. The lens aspect ratio (C) shows that mouse lenses are slightly wider at the lens equator. Lens volume (D), nuclear diameter (E), nuclear volume (F) and nuclear fraction (G) progressively increase with age. **, p <0.01. Please click here to view a larger version of this figure.

Discussion

There are several key considerations when using this method to measure lens stiffness. First, the coverslips are applied to the lens at a slightly oblique angle (8 - 8.5°) with respect to the bottom of the chamber (θ). This will apply a very small component of the load equatorially rather than axially. However, this equatorial load is considered negligible because $\sin \theta \approx 0.1$[19]. If this method is adapted for larger lenses, the angle of the coverslips to the bottom of the chamber would need to be measured to determine whether equatorial load should be factored into strain calculations. Second, it is crucial to allow the lens to equilibrate after the addition of each coverslip. The waiting period of 2 minutes allows time-dependent deformation (*i.e.*, creep) to occur, such that pictures are only taken when the lens is at an equilibrium shape[19]. Third, this protocol is optimized for measuring compressive strain on mouse lenses across a wide dynamic range of loads. In pilot studies, an applied load of 1,293 mg (*i.e.*, ten 18 x 18 mm coverslips) compressed the mouse lens to a maximum strain, beyond which increased loads do not cause appreciable further deformation. This is due to the presence of the rigid lens nucleus that does not deform appreciably under compression[19]. Fourth, this protocol avoids irreversible tissue damage. In previously published experiments, no changes in the mechanical properties of mouse lenses were observed upon repeat loading, suggesting that this method does not damage the lens[19]. When mechanically testing lenses of a different species or mutant lenses, pilot tests should be done to determine the maximum load needed for maximum strain by repeating steps 2.8 - 2.10 and comparing the strain-load curves, lens diameters and lens volumes between the first and second loading. Finally, this method provides an empirical measurement of the stiffness of the whole lens and cannot differentiate the contributions of different cell types (epithelial cells, cortical fibers, nuclear fibers) and the lens capsule to whole-lens mechanical properties.

The axial and equatorial strains are plotted here as functions of the imposed load. Previous studies have quantified mouse lens stiffness[19,21], resilience[21] or the change in diameter[18] upon applied load. Strain is a dimensionless quantity that allows direct comparison between lenses of different sizes. Note that equatorial extension (positive strain) occurs concurrently with the applied axial compression (negative strain) due to conservation of lens volume (*i.e.*, Poisson effect). However, the observed equatorial strains were much smaller in absolute magnitude than the axial strains, indicating that this method has less resolution to detect small changes in equatorial strain as compared to axial strain.

In summary, this simple method with an easily assembled device for measuring mouse lens stiffness can be applied generally and widely in lens research to better understand how mutations in proteins, pathologies and/or aging affect lens stiffness. While mouse lenses do not accommodate, this method can still elucidate the proteins and age-related modifications that contribute to increased lens stiffness, and potentially contribute new knowledge to developing novel treatments for presbyopia.

Disclosures

The authors have nothing to disclose.

Acknowledgements

This work was supported by National Eye Institute Grant R01 EY017724 (VMF) and National Institute of Arthritis and Musculoskeletal and Skin Diseases Grant K99 AR066534 (DSG).

References

1. Lovicu, F. J., & Robinson, M. L. *Development of the ocular lens.* Cambridge University Press, (2004).
2. Piatigorsky, J. Lens differentiation in vertebrates. A review of cellular and molecular features. *Differentiation.* **19** (3), 134-153 (1981).
3. Glasser, A. Restoration of accommodation: surgical options for correction of presbyopia. *Clin Exp Optom.* **91** (3), 279-295 (2008).
4. Keeney, A. H., Hagman, R. E., & Fratello, C. J. *Dictionary of ophthalmic optics.* Butterworth-Heinemann, (1995).
5. Millodot, M. *Dictionary of optometry and visual science.* 7th edn, Elsevier/Butterworth-Heinemann, (2009).
6. Heys, K. R., Cram, S. L., & Truscott, R. J. Massive increase in the stiffness of the human lens nucleus with age: the basis for presbyopia? *Mol Vis.* **10** 956-963 (2004).
7. Heys, K. R., Friedrich, M. G., & Truscott, R. J. Presbyopia and heat: changes associated with aging of the human lens suggest a functional role for the small heat shock protein, alpha-crystallin, in maintaining lens flexibility. *Aging Cell.* **6** (6), 807-815 (2007).
8. Pierscionek, B. K. Age-related response of human lenses to stretching forces. *Exp Eye Res.* **60** (3), 325-332 (1995).
9. Glasser, A., & Campbell, M. C. Biometric, optical and physical changes in the isolated human crystalline lens with age in relation to presbyopia. *Vision Res.* **39** (11), 1991-2015 (1999).
10. Weeber, H. A., & van der Heijde, R. G. On the relationship between lens stiffness and accommodative amplitude. *Exp Eye Res.* **85** (5), 602-607 (2007).
11. Weeber, H. A. *et al.* Dynamic mechanical properties of human lenses. *Exp Eye Res.* **80** (3), 425-434 (2005).
12. Fisher, R. F. Elastic properties of the human lens. *Exp Eye Res.* **11** (1), 143 (1971).
13. Krueger, R. R., Sun, X. K., Stroh, J., & Myers, R. Experimental increase in accommodative potential after neodymium: yttrium-aluminum-garnet laser photodisruption of paired cadaver lenses. *Ophthalmology.* **108** (11), 2122-2129 (2001).
14. Burd, H. J., Wilde, G. S., & Judge, S. J. An improved spinning lens test to determine the stiffness of the human lens. *Exp Eye Res.* **92** (1), 28-39 (2011).
15. Glasser, A., & Campbell, M. C. Presbyopia and the optical changes in the human crystalline lens with age. *Vision Res.* **38** (2), 209-229 (1998).
16. Pau, H., & Kranz, J. The increasing sclerosis of the human lens with age and its relevance to accommodation and presbyopia. *Graefes Arch Clin Exp Ophthalmol.* **229** (3), 294-296 (1991).
17. Hollman, K. W., O'Donnell, M., & Erpelding, T. N. Mapping elasticity in human lenses using bubble-based acoustic radiation force. *Exp Eye Res.* **85** (6), 890-893 (2007).
18. Baradia, H., Nikahd, N., & Glasser, A. Mouse lens stiffness measurements. *Exp Eye Res.* **91** (2), 300-307 (2010).
19. Gokhin, D. S. *et al.* Tmod1 and CP49 synergize to control the fiber cell geometry, transparency, and mechanical stiffness of the mouse lens. *PLoS One.* **7** (11), e48734 (2012).
20. Sindhu Kumari, S. *et al.* Role of Aquaporin 0 in lens biomechanics. *Biochem Biophys Res Commun.* (2015).
21. Fudge, D. S. *et al.* Intermediate filaments regulate tissue size and stiffness in the murine lens. *Invest Ophthalmol Vis Sci.* **52** (6), 3860-3867 (2011).
22. Kuszak, J. R., Mazurkiewicz, M., & Zoltoski, R. Computer modeling of secondary fiber development and growth: I. Nonprimate lenses. *Mol Vis.* **12,** 251-270 (2006).
23. Scarcelli, G., Kim, P., & Yun, S. H. In vivo measurement of age-related stiffening in the crystalline lens by Brillouin optical microscopy. *Biophys J.* **101** (6), 1539-1545 (2011).

